Depolarization and bonding in quasi-one-dimensional Na structures on Cu(001)

Guido Fratesi*

ETSF, CNISM, and Dipartimento di Scienza dei Materiali, Università di Milano-Bicocca, Via Cozzi 53, I-20125 Milano, Italy

(Received 13 July 2011; revised manuscript received 28 September 2011; published 14 October 2011)

The formation of quasi-one-dimensional (Q1D) $p(n \times 2)$-Na/Cu(001) structures is addressed by density-functional theory investigations for adsorbate coverage from low to the saturation one. A general dependence of the dipole moment on the given configuration is deduced by extending that for uniform distributions, and greatly affects the energetics of the Na overlayer. Larger stability for Q1D arrangements aligned along [110] and [1$\bar{1}$0] holds at coverage larger than 0.2 ML, in agreement with low-temperature He scattering experiments, and can be explained by a reduced dipole-dipole repulsion for the $p(4 \times 2)$ with respect to hexlike distributions. Interatomic bonding charge displacements along zigzag rows of Na atoms further support the Q1D structure and contribute significantly to the surface corrugation as seen by the He probe.

DOI: 10.1103/PhysRevB.84.155424 PACS number(s): 68.43.Fg, 73.20.−r, 71.15.Mb, 68.49.Bc

I. INTRODUCTION

Quasi-one-dimensional (Q1D) structures of adatoms at surfaces attract strong interest for the peculiar features brought by low dimensionality.[1,2] Their bottom-up self-assembly is particularly intriguing and can proceed by atom evaporation on anisotropic substrates, where the broken symmetry may derive, e.g., from the chosen surface cleavage angle[3] or can be induced by the presence of step edges.[1,4–7] Differently, organization onto Q1D structures may be driven by charge-density wave transition as, for example, those exhibited by several p (Ref. 8) and d (Refs. 2 and 5) systems.

Alkali metals may also give rise to Q1D structures, offering s-type electron states more delocalized and free-electron-like than those in p or d systems. Quantum well states can also be present, confined at the surface,[9] and alkali-adatom chains can provide electronic features typical of 1D metals.[10,11] As strong dipole-dipole repulsion between the atoms[12] promotes the formation of hexagonal overlayers, a requirement to be met is that the local substrate bonding overcomes such repulsion. Hence lighter alkali metals, having a smaller dipole moment upon adsorption and feeling a larger substrate potential, are more probable to arrange themselves into Q1D structures than the heavier ones. Nanometric lithium wires have been observed on the Cu(001) surface close to saturation coverage, where they coexist with narrow $c(2 \times 2)$ domains.[13–16] Recent investigations[17] have shown that wires are stabilized by a remarkable depolarization of the Li atoms and by the formation of Li-Li bonds along the structure. Bonding charges produce significant enhancements of surface corrugation and can be observed by helium atom scattering (HAS) experiments.

The formation of ordered Na/Cu(001) structures was also studied by HAS at low temperatures ($T_s = 50$ K).[18] At low coverage Θ, disordered hexagonal arrangements produced rings in diffraction patterns up to $\Theta = 0.125$ monolayer (ML) where domains of an ordered $c(4\sqrt{2} \times 2\sqrt{2})R45^\circ$ could be observed; next, ordering into a $\begin{pmatrix} 3 & 0 \\ -2 & 2 \end{pmatrix}$ array was found at $\Theta = 0.167$ ML, both with hexlike symmetry. Q1D structures were instead observed at $\Theta = 0.25$ ML and above and assigned to grouping of Na adatoms, the Cu(001) reconstruction being unlikely. At that coverage, very intense diffraction peaks indicated a large surface corrugation as seen by the He atom; eventually, at saturation (0.5 ML) a well-ordered and low-corrugated $c(2 \times 2)$ arrangement is formed. It is therefore interesting to understand the basic mechanisms of the ordering into such structures, especially concerning depolarization and interadsorbate bonding which were recently shown for the Li case.

In this paper the formation of submonolayer Na/Cu(001) structures is addressed by first-principles simulations. We determine the energetics of different overlayer configurations with coverage ranging between $\Theta = 0.06$ and 0.5 ML and identify the onset, as a function of Θ, of Q1D stability over arrays of evenly distributed (ED) Na atoms, still influenced by the substrate holding potential. The magnitude of the Na dipole moment is studied in order to identify the contribution of dipole-dipole repulsion to the adsorption energy of the overlayer. A simple depolarization formula is found to be valid for all structures up to overlayer saturation and provides work-function changes in very good agreement with experiments. Many similarities to the Li/Cu(001) case can be pointed out but Na depolarization is much less efficient than for Li, resulting in a larger residual interadsorbate interaction.

The outline of the paper is as follows. In Sec. II the theoretical and numerical method is described. In Sec. III we present our results for the adsorption energies and dipole moment of two classes of Na overlayers, as a function of coverage. We then discuss in detail the formation of the Q1D structures and a comparison to other alkali metals in Sec. IV. Finally, Sec. V is devoted to conclusions.

II. THEORETICAL METHOD

Coordinates and energies were determined within density-functional theory (DFT)[19,20] and the Perdew-Burke-Ernzerhof generalized gradient approximation (PBE-GGA)[21] by using the plane-wave pseudopotential code in the QUANTUM-ESPRESSO simulation package.[22] We have taken a slab with five Cu layers and single-side Na adsorption with dipole-field correction.[23] Dense $\mathbf{k}_{||}$-point meshes were adopted, equivalent to at least a 20×20 grid in the surface Brillouin zone of Cu(001). Other numerical parameters are equivalent to those adopted in our previous study for the potential-energy surface of the alkali-atom series.[24]

The adsorption energy (per Na atom) is evaluated as

$$E^{\rm ads} = \frac{E^{\rm tot}_{\rm Na/Cu(001)} - E^{\rm tot}_{\rm Cu(001)} - N E^{\rm tot}_{\rm Na}}{N}, \quad (1)$$

where $E^{\rm tot}_{\rm Na/Cu(001)}$, $E^{\rm tot}_{\rm Cu(001)}$, and $E^{\rm tot}_{\rm Na}$ are the structurally optimized total energies of the given Na/Cu(001) overlayer containing N Na atoms, of the clean surface, and of an isolated Na atom, respectively. It can be split in the following sum:

$$E^{\rm ads} = E^{\rm ads}_0 + E^{\rm int}. \quad (2)$$

Here $E^{\rm ads}_0$ is the single-adsorbate limit of $E^{\rm ads}$, and $E^{\rm int}$ contains by definition all kinds of interactions among the Na overlayer, both direct and substrate mediated. In particular, we will separate from $E^{\rm int}$ the contribution due to pairwise dipole-dipole repulsion within the overlayer, and call E' the residual interaction energy:

$$E^{\rm int} = E^{\rm dip} + E'. \quad (3)$$

In the point-dipole approximation, we have

$$E^{\rm dip} = \frac{1}{2}\sum_{ij} \frac{2\mu_i\mu_j}{|\mathbf{R}_i - \mathbf{R}_j|^3} \Big/ N, \quad (4)$$

where the sum runs over all couples of Na atom coordinates $\mathbf{R}$ in the overlayer (with $i \neq j$), μ_i is the electric dipole moment of adatom i, and the interaction with image dipoles is considered[12] (Hartree atomic units are adopted here and in the following unless differently specified). In order to validate the use of Eq. (4) it is worth noticing that the point-dipole approximation was shown to account very effectively for pairwise interactions between Na atoms at 0.08 ML, down to Na-Na separations such as those in the $c(2\times 2)$ structure.[25] We also found that the spatial distribution of the bonding charge at $\Theta = 0.25$ ML is still very similar to that for isolated adsorbates; the major difference with coverage increasing up to saturation is that regions of depleted density localize more between Na atoms.[26] Dipolar interactions are often the only ones considered in studies of adsorbed alkali-metal systems based on molecular-dynamics simulations,[27–30] successfully explaining several features of HAS experiments. We recall that oscillating Lau-Kohn interactions[31] may be more relevant than dipole-dipole ones to describe T-mode frequency dependence of Na/Cu(001) on Θ at low coverage.[32]

When the overlayer consists of equivalent Na atoms, the atom-specific dipole moment can be replaced by its average value μ, which we evaluate by our DFT simulations (otherwise, this will be taken as an approximation). This allows one to write

$$E^{\rm dip} \approx \mu^2 \frac{1}{N}\sum_i S_i \equiv \mu^2 S, \quad (5)$$

where

$$S_i = \sum_j R_{ij}^{-3} \quad (6)$$

and

$$S = \frac{1}{N}\sum_i S_i. \quad (7)$$

The quantity S_i, which has also been taken as a measure of the local adsorbate concentration,[28] additionally yields the electric field $\mathcal{E}_i$ acting on a dipole at site i due to all other dipoles. Again in the point-dipole approximation, we have[25]

$$\mathcal{E}_i = \sum_j \mu_j R_{ij}^{-3} \approx \mu S_i. \quad (8)$$

Such an electric field then acts self-consistently against the Na dipole, so that (to first order in $\mathcal{E}$)

$$\mu = \mu_0 - \alpha\mathcal{E} = \mu_0/(1+\alpha S), \quad (9)$$

where μ_0 is the dipole moment in the limit to zero coverage and α represents the adatom polarizability. We will also include effects up to the second order in the electric field by writing

$$\mu = \mu_0 - \alpha\mathcal{E} - \beta\mathcal{E}^2 \approx \frac{\mu_0}{1+\alpha S} - \frac{\beta S^2\mu_0^2}{(1+\alpha S)^3}. \quad (10)$$

This expression can be thought of as a linear dependence of the polarizability on $\mathcal{E}$, but it will implicitly account for other effects like wave-function overlap ones[33] as the interadsorbate distance reduces. The resulting work-function reduction by the overlayer is then evaluated as $\Delta\Phi = 4\pi\mu\Theta/A$, A being the area of the surface unit cell.

To compare with surface corrugations as probed by HAS experiments, we take a classical description of the scattering process and evaluate the classical turning point (CTP) of the He atom as a function of the surface coordinate, that is, the distance $z^{\rm CTP}(x,y)$ at which the He-surface potential $V(x,y,z)$ equals the incoming kinetic energy $E^{\rm kin}$ projected along the normal to the surface. Similarly to our previous studies,[30,34,35] we have adopted the effective-medium theory (EMT) and assumed that V is proportional to the electron density of the sample ρ at the position of the He atom, the proportionality constant being 45 eV Å^3.[36–38]

III. RESULTS

The most relevant structures investigated in this work are depicted in Fig. 1. We have considered two main sets. The first one (ED) mainly includes Na in hex-type or square arrays of hollow sites, where the Na-Na distance is maximized; see Figs. 1(a)–1(g) for structures hereby indicated as $\mathcal{S}_a$-$\mathcal{S}_g$. This also includes the $c(4\sqrt{2}\times 2\sqrt{2})R45^\circ$ ($\mathcal{S}_b$) and the $\left(\begin{smallmatrix}3 & 0\\ -2 & 2\end{smallmatrix}\right)$ ($\mathcal{S}_c$) cases proposed on the basis of He diffraction measurements.[18] The second set (Q1D), see Figs. 1(h)–1(l), consists of $p(n\times 2)$ structures where Na atoms form zigzag rows aligned along [110] or [1$\bar{1}$0]. These extend the $p(4\times 2)$ and $p(3\times 2)$ ones ($\mathcal{S}_k$ and $\mathcal{S}_l$) previously suggested.[18] Additionally, in Figs. 1(m)–1(t) other structures are shown to be examined later, including a quasi-one-dimensional 0.375-ML case ($\mathcal{S}_m$) previously proposed.[18]

Let us start by discussing the adsorption energy for the set of ED structures, which are collected in Table I together with the Na dipole moment. As coverage increases, the adsorption strength decreases rapidly and monotonically, as can be seen in Fig. 2(a). This is consistent with the fact that no condensation of the overlayer into larger coverage islands has been observed,[18] as instead found, e.g., for Na/Al(001); there, Na condenses into $c(2\times 2)$ islands already at $\Theta = 0.2$ ML.[39]

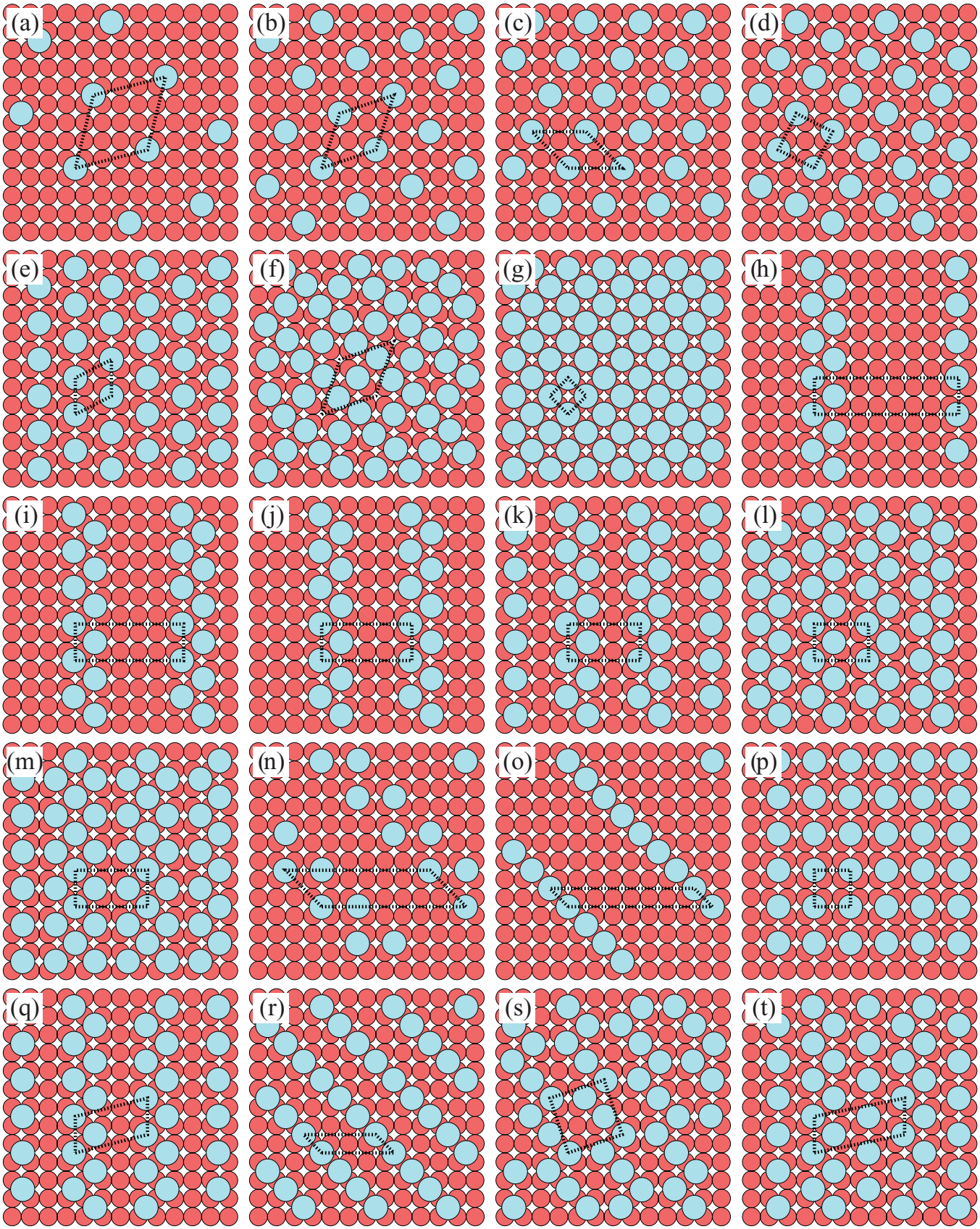

FIG. 1. (Color online) Top view of Na overlayer structures simulated in this work. Panels (a) to (t) show the optimized geometry for structures $\mathcal{S}_a$ to $\mathcal{S}_t$, as referred to in the text. Cyan (large bright) and red (small dark) circles stand for Na adatoms and surface Cu, respectively. Dashed lines indicate the unit cells taken for the calculations.

TABLE I. Coverage (Θ), adsorption energy ($E^{\rm ads}$), surface lattice vectors ($\mathbf{a}_1$ and $\mathbf{a}_2$), average dipole moment (μ), value of S [see Eq. (6)], interaction energy $E^{\rm int}$ and its decomposition into dipole ($E^{\rm dip}$) and other (E') contributions, and substrate deformation energy ($E^{\rm def}$), for structures investigated in this paper and depicted in Fig. 1.

Structure	Θ (ML)	$\begin{pmatrix}\mathbf{a}_1\\ \mathbf{a}_2\end{pmatrix}$	$E^{\rm ads}$ (eV)	μ (D)	S (eV/D^2)	$E^{\rm int}$ (eV)	$E^{\rm dip}$ (eV)	E' (eV)	$E^{\rm def}$ (eV)
ED:									
$\mathcal{S}_a$	0.067	$\begin{pmatrix}4&1\\1&4\end{pmatrix}$	−1.661	3.35	0.006	0.077	0.063	0.014	0.006
$\mathcal{S}_b$	0.125	$\begin{pmatrix}3&1\\1&3\end{pmatrix}$	−1.592	2.85	0.015	0.146	0.118	0.028	0.006
$\mathcal{S}_c$	0.167	$\begin{pmatrix}3&0\\-2&2\end{pmatrix}$	−1.549	2.45	0.023	0.189	0.138	0.051	0.009
$\mathcal{S}_d$	0.200	$\begin{pmatrix}1&2\\-2&1\end{pmatrix}$	−1.524	2.18	0.030	0.214	0.141	0.073	0.008
$\mathcal{S}_e$	0.250	$\begin{pmatrix}2&1\\0&2\end{pmatrix}$	−1.500	1.77	0.041	0.238	0.129	0.109	0.008
$\mathcal{S}_f$	0.375	$\begin{pmatrix}3&1\\1&3\end{pmatrix}$	−1.474	1.00	0.080	0.264	0.080	0.184	0.009
$\mathcal{S}_g$	0.500	$\begin{pmatrix}1&1\\-1&1\end{pmatrix}$	−1.455	0.67	0.117	0.283	0.052	0.231	0.004
Q1D $p(n\times 2)$:									
$\mathcal{S}_h$	0.125	$\begin{pmatrix}8&0\\0&2\end{pmatrix}$	−1.549	1.93	0.038	0.189	0.141	0.048	0.013
$\mathcal{S}_i$	0.167	$\begin{pmatrix}6&0\\0&2\end{pmatrix}$	−1.538	1.80	0.041	0.200	0.134	0.066	0.011
$\mathcal{S}_j$	0.200	$\begin{pmatrix}5&0\\0&2\end{pmatrix}$	−1.528	1.69	0.045	0.210	0.128	0.083	0.011
$\mathcal{S}_k$	0.250	$\begin{pmatrix}4&0\\0&2\end{pmatrix}$	−1.511	1.51	0.051	0.227	0.117	0.109	0.010
$\mathcal{S}_l$	0.333	$\begin{pmatrix}3&0\\0&2\end{pmatrix}$	−1.489	1.19	0.066	0.249	0.095	0.155	0.009
Other:									
$\mathcal{S}_m$	0.375	$\begin{pmatrix}4&0\\0&2\end{pmatrix}$	−1.475	1.01	0.081	0.263	0.083	0.180	0.007
$\mathcal{S}_n$	0.125	$\begin{pmatrix}8&0\\-2&2\end{pmatrix}$	−1.574	2.61	0.019	0.164	0.132	0.032	0.008
$\mathcal{S}_o$	0.125	$\begin{pmatrix}8&0\\-1&1\end{pmatrix}$	−1.515	2.04	0.037	0.223	0.153	0.071	0.006
$\mathcal{S}_p$	0.250	$\begin{pmatrix}2&0\\0&2\end{pmatrix}$	−1.497	1.76	0.041	0.241	0.129	0.112	0.007
$\mathcal{S}_q$	0.250	$\begin{pmatrix}4&1\\0&4\end{pmatrix}$	−1.511	1.51	0.051	0.227	0.117	0.109	0.010
$\mathcal{S}_r$	0.250	$\begin{pmatrix}4&0\\-1&1\end{pmatrix}$	−1.471	1.54	0.053	0.267	0.124	0.143	0.006
$\mathcal{S}_s$	0.300	$\begin{pmatrix}3&1\\-1&3\end{pmatrix}$	−1.483	1.31	0.061	0.255	0.104	0.150	0.008
$\mathcal{S}_t$	0.300	$\begin{pmatrix}5&1\\0&2\end{pmatrix}$	−1.492	1.38	0.057	0.246	0.109	0.136	0.009

The zero-coverage limit of $E^{\rm ads}$ can be found by extrapolating $E^{\rm ads} - E^{\rm dip}$ to $\Theta = 0$,[24] resulting in $E_0^{\rm ads} = -1.738$, eV and allows us to estimate the interaction energy within the overlayer. That is always repulsive and increases monotonically with coverage, following $E^{\rm ads}$. It is plotted in Fig. 2(b), and decomposed according to Eq. (3). At low coverage, the dipole-dipole contribution dominates $E^{\rm int}$, increasing with Θ up to about 0.2 ML where it saturates, and eventually decreasing at larger Θ. This is a consequence of the reduced Na dipole moment, see Fig. 3(a), which overcompensates the increased overlayer density. The residual interaction energy E' increases monotonically with coverage, so that it amounts to about 33% of the total interaction energy already at $\Theta = 0.20$ ML, then becoming the most relevant contribution (50% at about 0.25 ML and up to 82% at 0.50 ML); see Fig. 2(b). This analysis points out that pairwise dipolar interactions are the dominant contribution to the total interaction energy of the overlayer only at very low coverage. A large contribution to E' should be identified in a nonpairwise interaction energy due to substrate bond sharing among the adatoms. This is properly a surface effect well taken into account by the slab approach already at five layers. We then mention that overlayer-induced substrate deformations are relatively small in all cases (see $E^{\rm def}$ in Table I), so that their contribution to E' is limited.

We now consider the Q1D structures, whose adsorption energy is also reported in Table I and Fig. 2(a). They are energetically unfavorable at low coverage (compare, e.g., the 0.125-ML structures $\mathcal{S}_h$ and $\mathcal{S}_b$) because both $E^{\rm dip}$ and E' are larger than for quasi-hexagonal arrangements. Indeed, differently than for ED cases, $E^{\rm dip}$ increases monotonically as $\Theta \to 0$ because short Na-Na distances are always present and the dipole moment keeps growing. Furthermore, the substrate bond sharing among the Na atoms is now more localized and hence contributes to E' to a larger extent, summed to the cost of Na displacement from the hollow site by 0.21 Å [about 0.005 eV (Ref. 24)] and to a larger substrate relaxation (see $E^{\rm def}$ in Table I). Q1D structures become more stable than the hexlike arrangements for $\Theta \geqslant 0.2$ ML. In particular, the observed[18] $\mathcal{S}_k$ (Q1D at 0.25 ML) is 0.011 eV, more convenient than the ED $\mathcal{S}_e$.

Let us evaluate in more detail the dependence of the Na dipole moment on coverage, reported in Fig. 3(a). Besides the well-known reduction at increasing coverage, which is very effective when approaching overlayer completion,[40] one notices that at the same value of Θ, μ is smaller for Q1D structures than for ED ones and approaches a different zero-coverage limit. We now show that the two different $\mu(\Theta)$ functional forms can instead be recast into a single $\mu(S)$ dependence, following Eq. (8), valid for any configuration we tested. Indeed, the value of S is always larger for Q1D structures than for ED ones, and a nonzero value is approached as $\Theta \to 0$; see Fig. 3(b). The same holds for the electric field acting against the Na dipole. Hence a common $\mu(S)$ dependence follows, as reported in Fig. 3(c). A fit of Eq. (9) at low coverage ($S \leqslant 0.04$ eV/D^2) gives $\mu_0 = 3.86$ D and $\alpha = 25.9$ D^2/eV (i.e., $\alpha = 105$ a.u., sometimes expressed as

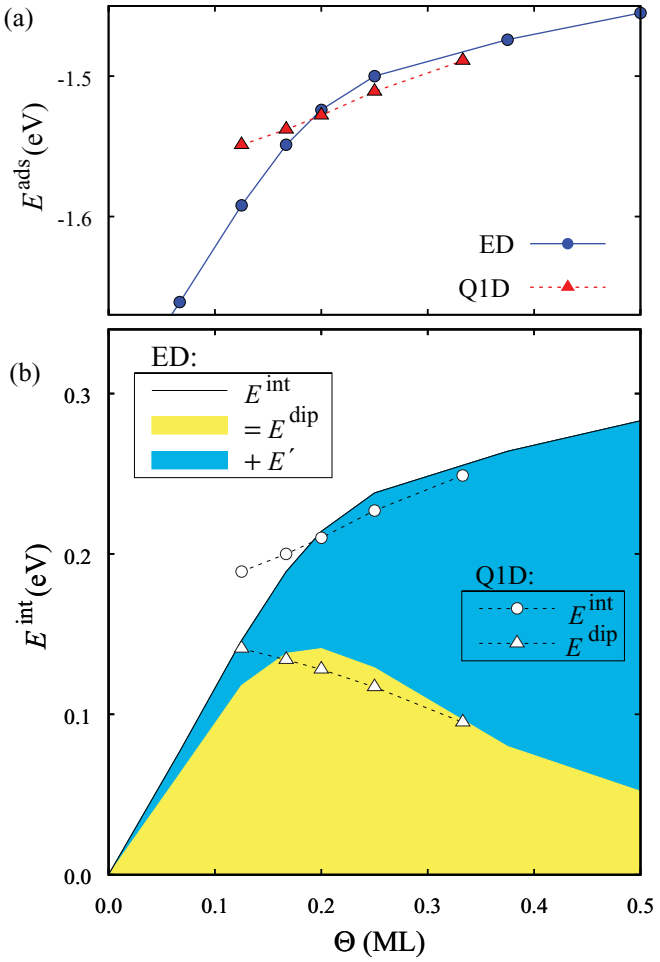

FIG. 2. (Color online) (a) Na adsorption energy E^{ads} for evenly distributed, see Figs. 1(a)–1(g), and quasi-one-dimensional structures, see Figs. 1(h)–1(l), as a function of coverage Θ. (b) Interaction energy E^{int} and its decomposition into dipole-dipole (E^{dip}) and other terms (E') for the same sets of configurations. In the ED case, filled areas sum up to the value of E^{int} indicated by the solid line. See the legend for the full explanation of symbols.

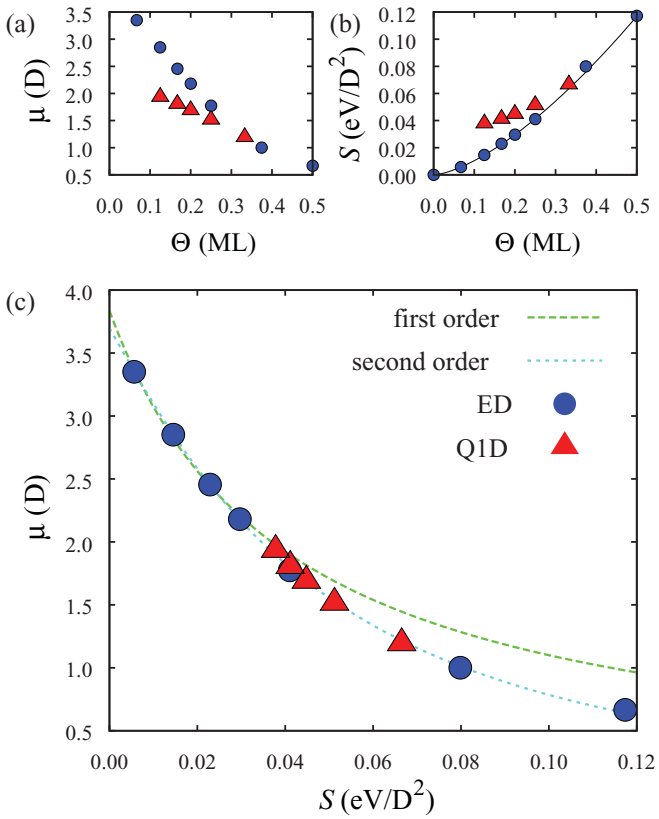

FIG. 3. (Color online) (a) Average dipole moment μ as a function of coverage Θ. (b) Quantity S; see Eq. (6). The solid line is for a hexagonal distribution. (c) Dependence of μ on S. Long and short dashed lines are fits considering a first- and second-order dependence of μ on the electric field, respectively; see Eqs. (9) and (10).

a volume, $\alpha = 15.5$ Å^3), the result being also reported in Fig. 3(c). This is not very different from $\mu_0 = 3.7$ D and $\alpha = 10$ Å^3, evaluated by keeping the coverage fixed in the simulations and by varying the distance of Na couples.[25] By fitting the second-order expression in the full coverage range, Eq. (10), we obtain $\mu_0 = 3.70$ D, $\alpha = 16.7$ D^2/eV, and $\beta = 83.2$ D^3/eV^2. Notice that much smaller values for μ_0 have been reported, namely $\mu_0 = 2.8$ D (and $\alpha = 17.7$ Å^3),[41] but the accuracy of our results is clearly supported by comparison to measured work-function changes, as shown in Fig. 4. Given the moderately high temperature in these experiments ($T_s = 180$ K),[14] where disordered hex-type arrangements were observed by low-energy electron diffraction (LEED), one has to compare the measurements to our results for ED structures (rather than those for Q1D ones), resulting in a very good agreement. No other *ab initio* calculation of the Na-coverage-dependent work function of Cu(001) has been proposed in the literature to our knowledge. The generality of the $\mu(S)$ dependence suggests that it can be adopted for studies where different coverages or local distributions of Na dipoles have to be taken into account, such as, for example, in molecular-dynamics simulations.

IV. DISCUSSION

A. Coverage-dependent stability of Q1D structures

In this section we analyze the energetics of Na structures and compare to low-temperature HAS observations by Graham *et al.*[18] Let us recall that, for Θ lower than about 0.1 ML, diffraction rings were observed, indicating the formation of quasihexagonal structures with no preferential orientation. More complex arrangements of diffraction peaks could be found at 0.125 ML, described by two domains of a $c(4\sqrt{2} \times 2\sqrt{2})R45^\circ$ structure ($\mathcal{S}_b$). The formation of the latter is driven by a combination of the substrate potential and repulsive interadsorbate interactions. This structure, with shortest Na-Na distances of 7.3 and 8.1 Å, is very effective in minimizing the dipole-dipole interaction with all adatoms in hollow sites: indeed, for a perfect hexagonal arrangement the value of S would be only 0.5% lower and that of E^{dip} no more than 1 meV lower. As a comparison, recall that the cost to move a Na adatom from the hollow to the bridge surface site is about 0.075 eV.[24,42] At that coverage, other structures with shorter Na-Na distances were also considered for the current study but found to have higher E^{ads}, consistent with experiments:

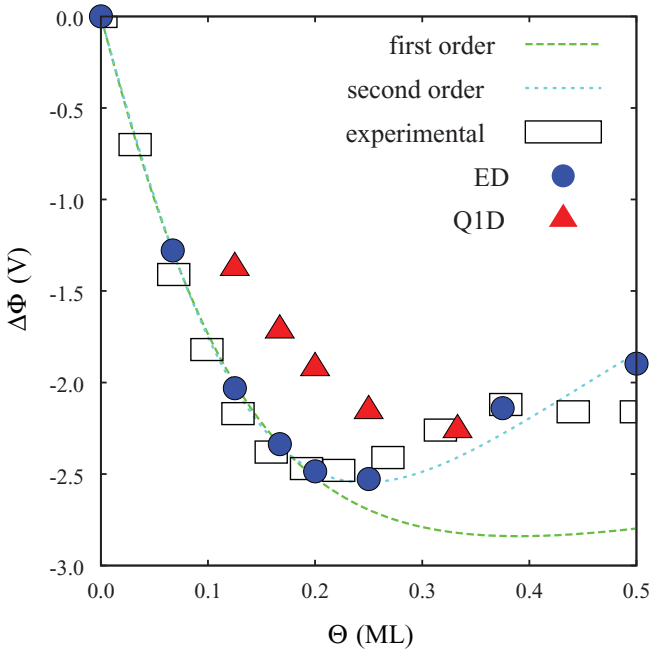

FIG. 4. (Color online) Coverage-dependent work-function reduction $\Delta\Phi$. Experimental data were taken at $T_s = 180$ K (Ref. 14). Long- and short-dashed lines refer to dipole moments computed according to Eqs. (9) and (10), respectively, and assuming a hexagonal distribution of Na adatoms.

one with third-nearest-neighbor adsorbates ($\mathcal{S}_n$) is higher by 0.018 eV; two with next-nearest neighbor, $\mathcal{S}_h$ and $\mathcal{S}_o$, are higher by 0.043 and 0.077 eV, respectively.

The picture is very different at a coverage twice as large, 0.25 ML, where $p(4 \times 2)$ diffraction patterns could be observed, and can be explained by virtue of the present results. Although the ED arrangement ($\mathcal{S}_e$) is also very efficient as for $E^{\rm dip}$ (again, no more than 1 meV higher with respect to the ideal case), the most stable structure we found is now the Q1D $\mathcal{S}_k$, indeed with $p(4 \times 2)$ periodicity, which is lower in energy by 0.011 eV. This is achieved by lowering $E^{\rm dip}$ through a reduction in the dipole moment (15% lower), which overcompensates the increased proximity of adsorbates (S increases by 24%). Other structures were simulated to focus on this especially interesting 0.25-ML case. First, a $p(2 \times 2)$ arrangement ($\mathcal{S}_p$): here, the dipole-dipole contribution is the same as in the hexlike arrangement $\mathcal{S}_e$, but a larger value of E' makes this structure 3 meV less convenient. Next, we considered a Q1D structure ($\mathcal{S}_q$), which, at variance with the $\mathcal{S}_k$ discussed above, is characterized by a different matching of the facing zigzag rows [see Fig. 1(q)]. Such modification does not affect (within 1 meV) the adsorption energy $E^{\rm ads}$ nor its contributions E' and $E^{\rm dip}$. Finally, we simulated a distribution of next-nearest-neighbor Na atoms with the adsorbates all lined up along [100] azimuths in a $p(2\sqrt{2} \times \sqrt{2})R45^\circ$ structure ($\mathcal{S}_r$). This is, however, 0.040 eV less stable than $\mathcal{S}_k$ mostly because of a large value of E' (0.143 eV), which could result from a much more localized sharing of Na-Cu bonds with respect to the zigzag case.

Increasing coverage further initially resulted in the observation of $p(3 \times 2)$ features in scattering experiments, which is compatible with the presence of $\mathcal{S}_l$ intermixed with $\mathcal{S}_k$.[18] Then, at 0.35 ML, strong Q1D 4×1 spots were observed in the diffraction patterns and attributed to the 0.375-ML structure here indicated as $\mathcal{S}_m$. In our calculations, $\mathcal{S}_m$ is almost equivalent energetically to $\mathcal{S}_f$, in which evenly distributed Na holes are created in the saturated overlayer. Always at 0.35 ML, weaker spots in diffraction experiments were assigned to a 0.30-ML arrangement, $\mathcal{S}_s$, with a $(\sqrt{10} \times \sqrt{10})R18.4^\circ$ unit cell.[18] We found, however, that such structure has an higher adsorption energy than arrangements both at lower ($\Theta = 0.25$, $\mathcal{S}_k$) and higher ($\Theta = 0.33$ ML, $\mathcal{S}_l$) coverage; see Table I. Conversely, always at 0.30 ML, we simulated a more stable $c(10 \times 2)$ configuration, where Na zigzag rows alternate narrow domains of ED atoms ($\mathcal{S}_t$), in analogy to the $c(5\sqrt{2} \times \sqrt{2})R45^\circ$-Li/Cu(001).[13,15–17] However, no experimental evidences for such a structure have been provided.

B. Overlayer bonding charge displacements

Despite the increased proximity of Na atoms in Q1D $\mathcal{S}_k$ vs ED $\mathcal{S}_e$ structures at 0.25 ML, which implies a stronger competition in the adatom-surface bonding, and the slightly larger contributions by structural displacements, we found the same value of E' (0.109 eV) in the two cases. This, together with the shorter Na-Na distance in $\mathcal{S}_k$, suggests the presence of bonding interactions along the chains, which we now highlight by reconsidering the surface corrugation as seen by the HAS experiments, in the light of our theoretical investigation. At the experimental setup (projected $E^{\rm kin} = 11$ meV),[18] the reflection condition for He atoms in the CTP-EMT description is given by $\rho(x,y,z^{\rm CTP}(x,y)) = 2.4 \times 10^{-4}$ Å^{-3}. Values of $z^{\rm CTP}(x,y)$ range from 3.5 to 6.5 Å above the surface layer of clean Cu(001), depending on structure and (x,y) coordinate. Contour levels of $z^{\rm CTP}(x,y)$ for structures $\mathcal{S}_b$, $\mathcal{S}_e$, $\mathcal{S}_k$, and $\mathcal{S}_m$ are reported in Figs. 5(a)–5(d), respectively. In agreement with HAS observations, structures $\mathcal{S}_b$, $\mathcal{S}_k$, and $\mathcal{S}_m$ are strongly corrugated ($\Delta z = \max z^{\rm CTP} - \min z^{\rm CTP} = 1.42$, 2.22, and 1.03 Å, respectively). Notice that density profiles for $\mathcal{S}_k$ and $\mathcal{S}_m$ are mostly corrugated only along [110], as observed. The exceptionally large Δz for $\mathcal{S}_k$, see also Fig. 5(e), is responsible for the very intense diffraction peaks in the experiments; conversely, the less stable ED structure at the same coverage, $\mathcal{S}_e$, would appear less corrugated, having $\Delta z = 0.39$ Å; see Fig. 5(b). We remark that the $c(2 \times 2)\mathcal{S}_g$ is flat on the scale of the figure ($\Delta z = 0.03$ Å).

The origin of the enhanced corrugation of the Q1D structure $\mathcal{S}_k$ with respect to the ED one $\mathcal{S}_e$, at 0.25 ML, is twofold. On the one hand, a larger portion of Cu surface is exposed between two Na rows in the Q1D case, so that $\min z^{\rm CTP}$ is lower (4.12 rather than 5.54 Å). On the other hand, a protrusion of density appears on top of the zigzag Na rows of the Q1D structure, therefore increasing $\max z^{\rm CTP}$ to 6.34 Å (5.93 Å for the ED structure). We now show that this second effect derives from bonding charge displacements within Na rows in the Q1D case. To see this, we partition the electron density of the Na/Cu system into the following sum:

$$\rho_{\rm Na/Cu(001)} = \rho_{\rm Cu(001)} + \sum_i \rho_{{\rm Na},i} + \sum_i \Delta\rho_{{\rm Na},i} + \Delta\rho. \quad (11)$$

Here, $\rho_{\rm Cu(001)}$ is the density of the clean surface; $\rho_{{\rm Na},i}$ is that of the neutral Na atoms; $\Delta\rho_{{\rm Na},i}$ is the well-known

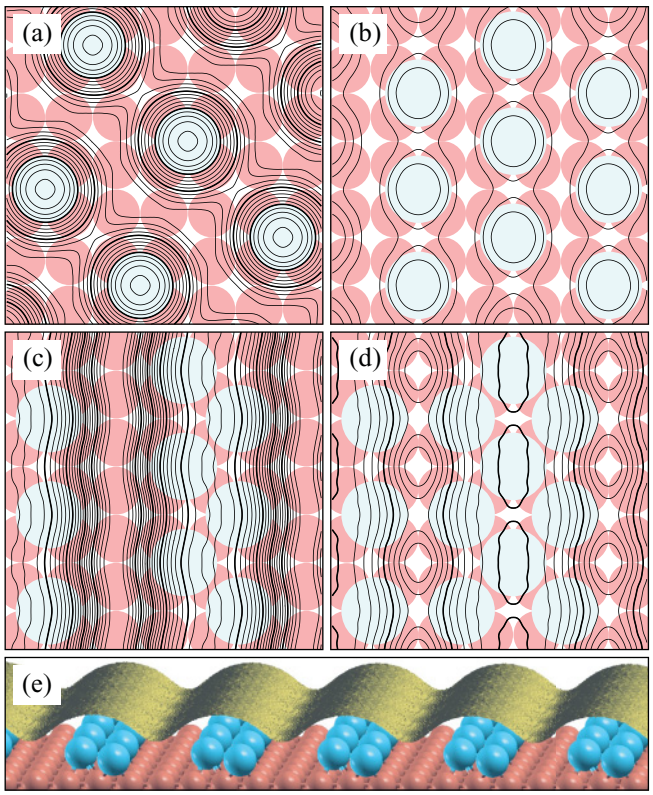

FIG. 5. (Color online) (a)–(d) Contour plot of the height of the electron density isosurface at $\rho = 2.4$ Å^{-3} (classical turning point for He with $E^{\mathrm{kin}} = 11$ meV). Thin (thick) height isolines are drawn every 0.1 Å (0.5 Å) starting from the minima (always occurring farthest from Na atoms). Panels (a)–(d) are for structures $\mathcal{S}_b$, $\mathcal{S}_e$, $\mathcal{S}_k$, and $\mathcal{S}_m$, respectively. (e) 3D view of the same electron density isosurface for $\mathcal{S}_k$.

charge displacement upon surface adsorption of individual adatoms,[24,26] see Fig. 6(a); finally, $\Delta\rho$ is a residual charge displacement due to mutual interaction among the adatoms forming the overlayer, which is of relevance here. Effects described in $\Delta\rho$ include the electron density backflow from below the adatom to above, consistent with the lowered dipole

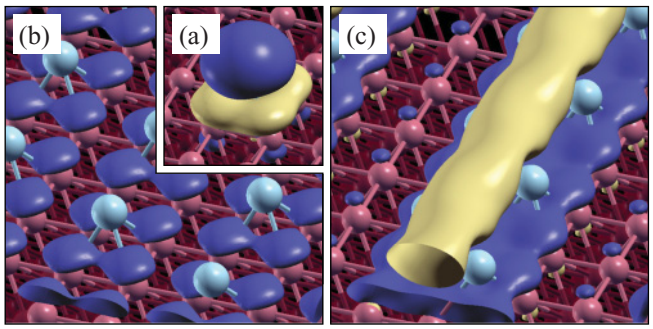

FIG. 6. (Color online) Electron density displacement upon Na adsorption and overlayer formation. Bright (dark) isosurfaces are for positive (negative) displacements of 5×10^{-3} Å^{-3}. (a) Electron density displacement for adsorbing a Na atom at 1/16 ML, $\Delta\rho_{\mathrm{Na},i}$. (b),(c) Residual charge displacements $\Delta\rho$ for structures $\mathcal{S}_e$ and $\mathcal{S}_k$, respectively. See Eq. (11) for the definition of all quantities, which were computed here by taking a (4×4) supercell with four Na atoms.

TABLE II. Coverage (Θ), adsorption energy (E^{ads}), average dipole moment (μ), and dipole-dipole interaction energy (E^{dip}) for K/Cu(001) structures analogous to the Na/Cu(001) ones depicted in Figs. 1(b), 1(n), 1(e), and 1(k).

Structure	Θ (ML)	E^{ads} (eV)	μ (D)	E^{dip} (eV)
$\mathcal{S}_b$	0.125	−1.574	3.93	0.225
$\mathcal{S}_n$	0.125	−1.542	3.58	0.238
$\mathcal{S}_e$	0.250	−1.414	1.88	0.145
$\mathcal{S}_k$	0.250	−1.391	1.83	0.145

moment. Additionally, in the case of $\mathcal{S}_k$ shown in Fig. 6(c), $\Delta\rho$ presents a 1D accumulation of density located in between the Na atoms, which is consistent with the formation of a metallic bond along the Q1D structure. That charge comes from a localized depletion of density from below. Conversely, in the case of $\mathcal{S}_e$ the density decrease close to the surface is evenly distributed above all Cu atoms, and the increase of density above Na so diffuse, not to reach the isovalue used for plotting in Fig. 6(b): no indication of direct interactions between Na pairs could be found.

The observation of bonding charges through HAS, as reported here, further points out how atom scattering experiments may critically depend on, and access to, the electronic properties of the sample. Other recent examples of this feature include effects related to the dynamics of the system. For example, the correlated diffusion of Na/Cu(001) resulted in a dependence on time of the electron density extension in vacuum, which could be misleadingly interpreted as a Na motion perpendicular to the surface;[28,34,35] the measurement of subsurface phonon dispersion curves on metals is made possible by phonon-induced electron-density displacements, which extend up to the surface.[43]

C. Comparison to other alkali-metal systems

The enhanced density protrusion observed for $\mathcal{S}_k$ is qualitatively and quantitatively similar to the one we recently pointed out for Li overlayers on Cu(001) upon condensation from 0.5 to 0.6 ML and formation of 1D Li wires.[17] Nevertheless, some differences have to be pointed out. In the Li case, a very large depolarization was found, Li atoms in the wires having a dipole moment (0.39 D) 41% smaller than that of Li atoms in coexisting $c(2 \times 2)$ domains. Here μ is only 15% smaller for the Q1D overlayer than for the ED one, and still significantly large (1.51 D). As a consequence, Na atoms in the row still feel strong repulsive forces, which displace them from the hollow sites to a Na-Na distance $d = 3.94$ Å, larger by 0.23 Å than that in bcc Na. Conversely, the same d as for the bulk alkali metal was found in the Li wires.

The next question is whether similar Q1D features could be observed at all for heavier alkali metals, starting from potassium. To answer this question, additional calculations were run for selected configurations of K/Cu(001) at 0.125 and 0.25 ML. The methodological setup is again the same as in Ref. 24, but for the denser Brillouin-zone sampling as mentioned in Sec. II for Na. Results are collected in Table II, following the same notation for the structures as given in Fig. 1. The adsorption of K on Cu(001) has been the subject of several studies mostly based on LEED, which show that

condensation into a $c(4 \times 2)$ ($\mathcal{S}_e$) is observed at $T_s = 130$ K starting from 0.2 ML (Ref. 44) [at room temperature and above, condensation to liquid islands was found from about 0.18 ML (Ref. 45)]. In agreement with these findings, our calculations for $\Theta = 0.25$ ML show that the ED structure $\mathcal{S}_e$ is favored over the Q1D $\mathcal{S}_k$ by 0.023 eV. The dipolar contribution to the interaction energy is the same in the two cases ($E^{\text{dip}} = 0.145$ eV). However, since K atoms in the zigzag row have a dipole moment only 3% smaller than in the hexlike case (1.83 and 1.88 D), their repulsion pushes them even farther from each other ($d = 4.82$ Å) than for Na in the same structure, and hence closer to the surface bridge site: the energy cost associated to this K displacement can be estimated as 0.020 eV (the potential-energy surface having a simple sinusoidal form and amounting to 0.031 eV in bridge[24]), accounting for most of the higher energy of this structure. At larger coverage, structures formed retain hexlike character; the system will follow a commensurate to incommensurate transition, eventually followed by rotation of the K overlayer with respect to the underlying Cu lattice.[46] A LEED investigation of K/Ni(001) also pointed out the possibility of Q1D ordering at low temperatures through uniaxial compression of the $c(4 \times 2)$ domains,[47] which, however, has not been reported yet for K/Cu(001). Given the larger covalent radius of K, one could also look at lower coverages for Q1D structures, possibly observable at very low T_s not hitherto considered in the experiments. However, the dipole moment then becomes even larger and we would not expect that such ordering could form, independently of surface temperature. As an example, taking $\Theta = 0.125$ ML, we have $\mu \approx 4$ D.[40] At that coverage we analyzed two arrangements, the hexlike $\mathcal{S}_b$ and $\mathcal{S}_n$ (which is a scaled and rotated analog of $\mathcal{S}_k$), finding that also in this case the hexlike distribution is lower in energy (by 0.032 eV).

V. CONCLUSIONS

We have studied the formation of quasi-one-dimensional Na/Cu(001) structures at low temperature, as a function of coverage. First-principles simulations provide a rationale for the structures previously observed by atomic diffraction and allow us to identify the coverage threshold ($\Theta \geqslant 0.20$ ML) where condensation of adsorbates into chains of next-nearest-neighbor Na atoms is energetically preferred, in agreement with experiments. Those configurations are stabilized by the enhanced depolarization of the overlayer and consequent reduction of dipole-dipole repulsion, which is more effective in this coverage range. At lower coverage hexlike arrangements are favored, although strongly influenced by the underlying substrate potential.

Coverage-dependent study of the dipole moment show that simulations are in very good agreement with work-function measurements; remarkably, a single functional dependence fits all computed data, and could be used to describe the dipole moment of arbitrary arrangements of Na atoms. We expect this property to hold generally for alkali-metal/metal systems.

As chains of next-nearest-neighbor Na atoms form in the $p(4 \times 2)$ structure, electron density accumulates in a 1D bonding feature in between adjacent adsorbates. This effect contributes to the large surface corrugation observed by HAS in presence of Q1D structures, and shows another case where atom scattering experiments, with the additional insight of first-principle investigations, are also a probe to the electronic properties of the sample.

The formation of Q1D Na/Cu(001) structures is to several aspects analogous to the formation of Li wires on the same substrate. Nevertheless, larger dipole moments are still present for Na, preventing interatomic distances typical of the alkali-metal as found for Li.

ACKNOWLEDGMENTS

Computational resources were made available by CINECA through the ISCRA initiative (Application No. HP10C7B0DN). I thank G. P. Brivio and M. I. Trioni for discussions.

*Also at Dipartimento di Fisica, Università degli Studi di Milano, via Celoria 16, I-20133 Milano, Italy.

[1] P. Gambardella, A. Dallmeyer, K. Maiti, M. C. Malagoli, W. E. K. Kern, and C. Carbone, Nature (London) **416**, 301 (2002).
[2] M. Grioni, S. Pons, and E. Frantzeskakis, J. Phys.: Condens. Matter **21**, 023201 (2009).
[3] A. Menzel, Z. Zhang, M. Minca, T. Loerting, C. Deisl, and E. Bertel, New J. Phys. **7**, 102 (2005).
[4] K. S. Kim, H. Morikawa, W. H. Choi, and H. W. Yeom, Phys. Rev. Lett. **99**, 196804 (2007).
[5] J. A. Lipton-Duffin, A. G. Mark, J. M. MacLeod, and A. B. McLean, Phys. Rev. B **77**, 125419 (2008).
[6] M. Bode, A. Kubetzka, O. Pietzsch, and R. Wiesendanger, Appl. Phys. A **72**, S149 (2001).
[7] S. Shiraki, H. Fujisawa, T. Nakamura, T. Muro, M. Nantoh, and M. Kawai, Phys. Rev. B **78**, 115428 (2008).
[8] T. Aruga, Surf. Sci. Rep. **61**, 283 (2006).
[9] J. M. Carlsson and B. Hellsing, Phys. Rev. B **61**, 13973 (2000).
[10] T. Aruga, H. Tochihara, and Y. Murata, Phys. Rev. Lett. **53**, 372 (1984).
[11] M. Tsukada, H. Ishida, and N. Shima, Phys. Rev. Lett. **53**, 376 (1984).
[12] W. Kohn and K. H. Lau, Solid State Commun. **18**, 553 (1976).
[13] H. Tochihara and S. Mizuno, Surf. Sci. **279**, 89 (1992).
[14] S. Mizuno, H. Tochihara, and T. Kawamura, Phys. Rev. B **50**, 17540 (1994).
[15] H. Tochihara and S. Mizuno, Prog. Surf. Sci. **58**, 1 (1998).
[16] D. A. MacLaren, C. Huang, A. C. Levi, and W. Allison, J. Chem. Phys. **129**, 094706 (2008).
[17] C. Huang, G. Fratesi, D. A. MacLaren, W. Luo, G. P. Brivio, and W. Allison, Phys. Rev. B **82**, 081413 (2010).
[18] A. P. Graham and J. P. Toennies, Phys. Rev. B **56**, 15378 (1997).
[19] P. Hohenberg and W. Kohn, Phys. Rev. B **136**, 864 (1964).
[20] W. Kohn and L. J. Sham, Phys. Rev. **140**, A1133 (1965).

[21] J. P. Perdew, K. Burke, and M. Ernzerhof, Phys. Rev. Lett. **77**, 3865 (1996).
[22] P. Giannozzi *et al*., J. Phys.: Condens. Matter **21**, 395502 (2009).
[23] L. Bengtsson, Phys. Rev. B **59**, 12301 (1999).
[24] G. Fratesi, Phys. Rev. B **80**, 045422 (2009).
[25] G. Fratesi, A. Pace, and G. P. Brivio, J. Phys.: Condens. Matter **22**, 304005 (2010).
[26] H. Ishida, Phys. Rev. B **42**, 10899 (1990).
[27] J. Ellis, A. P. Graham, F. Hofmann, and J. P. Toennies, Phys. Rev. B **63**, 195408 (2001).
[28] G. Alexandrowicz, A. P. Jardine, H. Hedgeland, W. Allison, and J. Ellis, Phys. Rev. Lett. **97**, 156103 (2006).
[29] A. P. Jardine, G. Alexandrowicz, H. Hedgeland, R. D. Diehl, W. Allison, and J. Ellis, J. Phys.: Condens. Matter **19**, 305010 (2007).
[30] H. Hedgeland, P. R. Kole, H. R. Davies, A. P. Jardine, G. Alexandrowicz, W. Allison, J. Ellis, G. Fratesi, and G. P. Brivio, Phys. Rev. B **80**, 125426 (2009).
[31] K. H. Lau and W. Kohn, Surf. Sci. **75**, 69 (1978).
[32] A. P. Graham, J. P. Toennies, and G. Benedek, Surf. Sci. **556**, L143 (2004).
[33] B. N. J. Persson and H. Ishida, Phys. Rev. B **42**, 3171 (1990).
[34] G. Fratesi, G. Alexandrowicz, M. I. Trioni, G. P. Brivio, and W. Allison, Phys. Rev. B **77**, 235444 (2008).
[35] M. I. Trioni, G. Fratesi, S. Achilli, and G. P. Brivio, J. Phys.: Condens. Matter **21**, 264003 (2009).
[36] J. K. Nørskov and N. D. Lang, Phys. Rev. B **21**, 2131 (1980).
[37] N. Esbjerg and J. K. Nørskov, Phys. Rev. Lett. **45**, 807 (1980).
[38] M. Manninen, J. K. Nørskov, M. J. Puska, and C. Umrigar, Phys. Rev. B **29**, 2314 (1984).
[39] E. Lundgren, A. Beutler, R. Nyholm, J. Andersen, and D. Heskett, Surf. Sci. **370**, 311 (1997).
[40] P. Senet, J. P. Toennies, and G. Witte, Chem. Phys. Lett. **299**, 389 (1999).
[41] A. Cucchetti and S. C. Ying, Phys. Rev. B **60**, 11110 (1999).
[42] A. P. Graham, F. Hofmann, J. P. Toennies, L. Y. Chen, and S. C. Ying, Phys. Rev. Lett. **78**, 3900 (1997).
[43] G. Benedek, M. Bernasconi, V. Chis, E. Chulkov, P. M. Echenique, B. Hellsing, and J. P. Toennies, J. Phys.: Condens. Matter **22**, 084020 (2010).
[44] M.-S. Chen, S. Mizuno, and H. Tochihara, Surf. Sci. **601**, 5162 (2007).
[45] T. Aruga, H. Tochihara, and Y. Murata, Surf. Sci. **158**, 490 (1985).
[46] T. Aruga, H. Tochihara, and Y. Murata, Phys. Rev. Lett. **52**, 1794 (1984).
[47] D. Fisher and R. D. Diehl, Phys. Rev. B **46**, 2512 (1992).